HHS Public Access

Author manuscript

Neuroimage. Author manuscript; available in PMC 2018 May 15.

Published in final edited form as:

Neuroimage. 2017 May 15; 152: 371–380. doi:10.1016/j.neuroimage.2017.02.074.

Functional Connectivity and Activity of White Matter in Somatosensory Pathways under Tactile Stimulations

Xi Wu[a,b,1], **Zhipeng Yang**[a,b,1], **Stephen K. Bailey**[c], **Jiliu Zhou**[a], **Laurie E. Cutting**[c,d,e], **John C. Gore**[b,f,g], and **Zhaohua Ding**[b,g,h,*]

[a]Department of Computer Science, Chengdu University of Information Technology, Chengdu, P.R. China, 610225

[b]Vanderbilt University Institute of Imaging Science, Nashville, TN, 37232

[c]Vanderbilt Brain Institute, Vanderbilt University, Nashville, TN, 37232

[d]Vanderbilt Kennedy Center, Vanderbilt University, Nashville, TN, 37232

[e]Peabody College of Education and Human Development, Vanderbilt University, Nashville, TN, 37232

[f]Department of Radiology and Radiological Sciences, Vanderbilt University Medical Center, Nashville, TN, 37232

[g]Department of Biomedical Engineering, Vanderbilt University, Nashville, TN, 37232

[h]Department of Electrical Engineering and Computer Science, Vanderbilt University, Nashville, TN, 37232

Abstract

Functional MRI has proven to be effective in detecting neural activity in brain cortices on the basis of blood oxygenation level dependent (BOLD) contrast, but has relatively poor sensitivity for detecting neural activity in white matter. To demonstrate that BOLD signals in white matter are detectable and contain information on neural activity, we stimulated the somatosensory system and examined distributions of BOLD signals in related white matter pathways. The temporal correlation profiles and frequency contents of BOLD signals were compared between stimulation and resting conditions, and between relevant white matter fibers and background regions, as well as between left and right side stimulations. Quantitative analyses show that, overall, MR signals from white matter fiber bundles in the somatosensory system exhibited significantly greater temporal correlations with the primary sensory cortex and greater signal power during tactile stimulations than in a resting state, and were stronger than corresponding measurements for background white matter both during stimulations and in a resting state. The temporal correlation

[*]Corresponding Author: Vanderbilt University Institute of Imaging Science, 1161 21st Avenue South, MCN AA-1105, Nashville, TN 37232-2310. Tel.: (615)322-7889; fax: (615)322-0734. zhaohua.ding@vanderbilt.edu.

[1]These authors contribute equally to this work.

and signal power under stimulation were found to be twice those observed from the same bundle in a resting state, and bore clear relations with the side of stimuli. These indicate that BOLD signals in white matter fibers encode neural activity related to their functional roles connecting cortical volumes, which are detectable with appropriate methods.

Keywords

White matter; functional MRI; sensory stimulation; diffusion MRI

1 INTRODUCTION

Functional magnetic resonance imaging (fMRI) is well established as a primary neuroimaging technique for detecting neural activities in the human brain. Based on blood oxygenation level dependent (BOLD) signal changes associated with hemodynamic responses to stimuli, fMRI has been widely used to localize and quantify regional activities and to assess synchronous activities across time (Ogawa et al., 1990; Biswal et al., 1995; Gore, 2003; Fox and Raichle, 2007). However, the tremendous successes over the past quarter of a century have focused on studies of cortical gray matter, and the detection of functional activities in white matter has rarely been reported in the literature. The paucity of reports on white matter activities is presumably partly attributed to the much lower blood flow and volume in white matter (Nonaka et al., 2003a & 2003b), and therefore much lower BOLD signal changes than in gray matter consistent with lower metabolic demands.

We have recently reported our observations that MRI signals from T_2*-sensitive acquisitions in a resting state exhibit structure-specific anisotropic temporal correlations in white matter (Ding et al., 2013; Ding et al., 2016). Based on these observations, we proposed a concept of spatio-temporal correlation tensors that characterize correlational anisotropy in white matter BOLD signals. Moreover, we found that directional preferences of spatio-temporal correlation tensors along many white matter tracts are grossly consistent with those revealed by diffusion tensors, and that evoked functions selectively enhance visualization of relevant fiber pathways. These tend to suggest that BOLD signals in white matter may encode neural activity as well, and may be detectable using appropriately sensitive imaging and analysis techniques such as improved imaging hardware (Mazerolle et al., 2013), pulse sequences (Gawryluk et al., 2009), stimulation and analysis strategies (Tettamanti et al, 2002; Weber et al., 2005; D'Arcy et al., 2006; Yarkoni et al., 2009; Marussich et al., 2016).

Over a decade ago, despite the presence of large differences in vascular density between gray matter and white matter, the oxygen extraction fraction was shown to be relatively uniform throughout the parenchyma of a resting brain (Raichle et al., 2001). Furthermore, the BOLD signal changes in white and gray matter in response to hypercapnia are largely comparable when normalized with regional cerebral blood flow (Rostrup et al., 2000). We have observed that BOLD signals in a resting state exhibit similar temporal and spectral profiles in both gray and white matter of the human brain (Ding et al., 2013), and that their relative low frequency (0.01–0.08 Hz) signal powers are comparable (Ding et al., 2016). In addition, our recent experiments with anesthetized squirrel monkeys demonstrate that low

frequency activity in both gray and white matter vary similarly with the level of anesthesia (Wu et al., 2016). Taken together, these findings converge to support the view that variations in BOLD signals that are believed to reflect neural activities in gray matter may also be detectable in white matter.

In this work, we further explore BOLD signal properties in brain white matter under functional loading. We hypothesize that functional loading should enhance the detectability of BOLD signals along white matter pathways that are relevant to specific evoked functions. To examine this hypothesis we imaged a cohort of normal human subjects subject to tactile stimulation of the palm, and then analyzed the temporal and frequency profiles of BOLD signal fluctuations in the somatosensory system. We specifically investigated whether there are significant temporal correlations in BOLD signals between the primary somatosensory cortex and projection pathways that are connected to it, and whether there are common signal characteristics that are shared between them. We compared the results of somatosensory stimulations to both palms, and to resting conditions. In particular, we used conventional stimulus-evoked functional MRI to identify cortical volumes in the primary somatosensory system. We used separate diffusion MRI acquisitions to identify relevant white matter tracts between these regions and thalamus and pons. We then examined the task and resting state correlations between the BOLD signals from the cortical volumes and the white matter tracts and compared them to volumes in white matter elsewhere.

2 METHODS

2.1 Data acquisition

Full brain MRI data were acquired from twelve healthy (six males and six females), and right-handed adult volunteers (mean age = 27.8 yrs, stdev = 4.8 yrs). No subjects had a history of neurological, psychiatric or medical conditions as determined by interview. Prior to imaging, informed consent was obtained from each subject according to protocols approved by the Vanderbilt University Institutional Review Board. All imaging was performed on a 3T Philips Achieva scanner (Philips Healthcare, Inc., Best, Netherlands) using a 32-channel head coil.

Three sets of images sensitive to BOLD contrast were acquired using a T_2*-weighted (T_2*w) gradient echo (GE), echo planar imaging (EPI) sequence with TR=3 s, TE=45 ms, matrix size=80×80, FOV=240×240 mm^2, 34 axial slices of 3 mm thick with zero gap, and 145 volumes. During the same imaging session, diffusion weighted images (DWI) were obtained using a single-shot, spin echo EPI sequence with b=1000 s/mm^2, 32 diffusion-sensitizing directions, TR=8.5 s, TE=65 ms, SENSE factor=3, matrix size=128×128, FOV=256×256, 68 axial slices of 2 mm thick with zero gap. To provide anatomical references, 3D high resolution T_1-weighted (T_1w) images were also acquired using a multi-shot 3D GE sequence at voxel size of 1×1×1 mm^3. The order of image acquisitions was T_1w, resting state, tactile stimulations to the right palm, DWI and tactile stimulations to the left palm. The three functional runs had the same time duration of 435 seconds.

Sensory stimuli were prescribed in a block design format, which started with 30 seconds of palm stimulations by continuous brushing followed by 30 seconds of no stimulation, and so

on. Prior to administration of the stimuli, five volumes were acquired in a resting state. During the image acquisitions, subjects lay in a supine position with eyes closed (in resting state), or fixed on a cross in the middle of the screen (no stimulus) or on an arrow sign (with stimulus).

2.2 Image preprocessing

Once acquired, all BOLD time series were corrected for slice timing and subject's head motion, and subsequently smoothed with a Gaussian kernel at FWHM=4 mm using SPM12. The smoothed BOLD signals were then linearly detrended and normalized into unit variance voxel-wise. Meanwhile, diffusion tensors were fit from the DWI data using a least squares approach (Jones and Cercignani, 2010) with in-house software. Finally, the T_1w images were segmented into gray and white matter and cerebrospinal fluid images using SPM12, all of which, along with the original T_1w images, were co-registered with the b=0 DWI data individually for each subject.

2.3 Characterization of BOLD signals in time and frequency domains

BOLD signals were characterized in both the time and frequency domains. In the time domain, temporal correlations between the resting state and stimulus evoked BOLD signals from identified white matter tracts and those from the primary somatosensory cortex (S1) were analyzed. In the frequency domain, power spectra of the BOLD signals were computed for each voxel, and the magnitude of the frequency corresponding to the fundamental frequency of the periodic stimuli was determined, yielding three magnitude maps of stimulus frequency respectively for the three sets of T_2*w images acquired.

The S1 region was initially defined in MNI space as a combination of Brodman's areas (BA) 1, 2 and 3 in the postcentral gyrus of each hemisphere, using the PickAtlas tool (Maldjian et al., 2003) supplied with SPM12. The initial S1 was then transformed into the space of the BOLD data acquired with tactile stimulations to the contralateral palm. Finally, the transformed S1 region was multiplied by the magnitude map of the stimulus frequency and was thresholded at 80% maximum magnitude, to generate an activation adjusted S1 region. This process reduced false positives in the S1 region due to misregistration from the MNI space to the native space of individual subjects.

Within the S1 region defined above, the first principal component of all BOLD signal time courses was derived, with which three maps of Pearson linear correlations were computed:

M1: Correlations of BOLD data from left palm stimulations with S1 in right hemisphere

M2: Correlations of BOLD data from right palm stimulations with S1 in left hemisphere

M3: Correlations of BOLD data from resting state with S1in both hemispheres[2]

[2]In this map, the principal component of S1 was computed with the two hemispheres pooled together, with the S1 in each hemisphere "copied" from its corresponding activation adjusted region in the stimulated images by image co-registration.

Prior to computations of the correlations, all the BOLD signals were band-pass filtered to retain frequencies only of 0.01–0.08 Hz. This frequency band contained the principal stimulation frequency of 0.016Hz (and its low order harmonics). To suppress potential confounding signals from adjacent but functionally unrelated white matter fibers, we computed for each voxel the first two principal components (with largest factor loadings) within a window of three voxels in each spatial dimension and reconstructed the time series back using these two components. The correlation coefficients were computed between the reconstructed BOLD signals of all brain voxels and the first principal component of the BOLD signals within the S1 region defined above.

These three correlation maps were converted to absolute values and subsequently co-registered with the b=0 DWI data for each subject, along with the three magnitude maps of stimulus frequency.

2.4 Reconstruction of somatosensory fiber pathways

BOLD signals were analyzed from identified somatosensory fiber pathways, which were reconstructed from diffusion tensor data using a probabilistic tracking approach that was modified from Friman et al. (2006).

Definitions of regions of interest (ROI)—Our fiber tracking requires source and target ROIs to be specified. In this work, three ROIs in each hemisphere were defined, which included the S1, the thalamus and the base of the pons. The S1 volume was defined as in the preceding section; the thalamus and the base of the pons were defined similarly except that they were not multiplied by the magnitude map and the base of the pons was chosen to be its three most inferior slices.

To further improve the robustness of S1 and thalamus definitions, the S1 and thalamus regions transferred into the DWI space were multiplied by the gray matter image, and then eroded by one voxel using common morphological operations.

Fiber tracking—Probabilistic fiber tracking was implemented for each hemisphere separately, with the thalamus as the source ROI and the S1 or the base of the pons as the target ROI. To begin with, a voxel within the thalamus was randomly sampled, from which fiber tracking was launched. At each step of fiber tracking, the direction to proceed along was a randomly perturbed principal direction of the diffusion tensor. The tracking process was repeated 1000 times until it reached the target ROI or exceeded an allowable number of steps.

Two maps were computed from the fibers that successfully reached the target ROI: one was the map of probability density of fibers that traversed each voxel, i.e., the number of traversing fibers divided by the total number of successful fibers, and the other was the map of mean direction of all the fibers traversing each voxel. With these two maps, streamlines were backtracked from the target ROI by following the reverse direction in the direction map voxel-by-voxel with fiber probability density above a preset threshold of 0.1%.

Fiber bundle skeletonization—Streamlines generated by the backtracking process were first automatically clustered into fiber bundles using an algorithm we developed earlier (Ding et al., 2003). Within the largest fiber bundle, the mean magnitude of the BOLD signal at the stimulus frequency was calculated for each streamline, and the one with the largest mean was chosen as the bundle skeleton. Fig. 1 below shows the flowchart of fiber tracking and skeletonization processes and some representative skeletons:

Time and frequency analyses of BOLD signals were performed along the bundle skeleton. The maximum Pearson correlation coefficient to the S1 signals and magnitude of stimulus frequency within a distance of one voxel along the perpendicular direction of the skeleton at each side were projected onto it.

3 RESULTS

We measured the mean temporal correlation of BOLD signals between S1 and thalamus-S1 and ponto-thalamus (Pon-TH) bundles, and mean magnitude of BOLD signals at the stimulus frequency in these regions in both hemispheres for all the twelve subjects. The quantities were derived during resting state and during left palm and right palm stimulations respectively. The mean correlations were converted to Fisher's Z-scores for statistical testing, and two-tailed, paired students' t-tests were used to assess differences. To remove potential partial volume effects from gray matter, two voxels from each end of the bundle were excluded from statistical analysis.

Temporal correlations during tactile stimulations and in a resting state are compared in Fig. 2, which shows the mean correlation between signals along the skeleton of the bundle connecting the thalamus to S1 and the S1 region for all the twelve subjects studied. In this figure, the left column compares the mean correlation along the skeleton connecting the thalamus to S1 in the right hemisphere (TH-S1-R) and in the left hemisphere (TH-S1-L) during left palm stimulations as well as mean correlation along the TH-S1-R skeleton at rest (TH-S1-R-RS); the right column compares the corresponding mean correlation for the TH-S1-L and TH-S1-R skeletons during right palm stimulations as well as mean correlation along the TH-S1-L skeleton at rest (TH-S1-L-RS). Mean correlations from background[3] (BG) white matter under tactile stimulations and resting conditions were also included for comparisons. It can be seen that, during palm stimulations, the BOLD signals from bundle skeleton in the contralateral hemisphere exhibited significantly higher correlation than that in the resting state condition for 20 comparisons, and higher correlation than that in BG white matter both during tactile stimulations and in resting state condition (BG-RS) for all the comparisons. Furthermore, the mean correlation from palm stimulations was shown to be side-dependent: right palm stimulations increased the correlation along the TH-S1-L skeleton more than along the TH-S1-R skeleton in ten subjects, whereas left palm stimulations increased the correlation along the TH-S1-R skeleton more than along the TH-S1-L skeleton only in five subjects.

[3]Background included 1000 random white matter voxels outside the fiber bundles connecting thalamus to S1 and to pons. We chose 1000 random voxels because they tended to produce convergent mean and standard deviation of correlation coefficients.

Similar observations can also be inferred from Fig. 3, which shows the mean correlation between the S1 and the skeleton of the bundle connecting pons to thalamus (Pon-TH-R and Pon-TH-L) for all the twelve subjects studied. During palm stimulations, the bundle skeleton in the contralateral hemisphere exhibited significantly higher correlation with S1 than that in the resting state condition (Pon-TH-R-RS and Pon-TH-L-RS) for 20 comparisons, and higher correlation than that of BG white matter during tactile stimulations for 21 comparisons and in a resting state for 20 comparisons. However, in contrast to the thalamus-S1 skeletons, both left and right palm stimulations significantly increased the mean correlation along the contralateral ponto-thalamus skeleton in only five subjects studied.

Quantitative analysis of the twelve subjects is summarized in Tab. 1 and 2. As can be seen from Tab. 1, the mean temporal correlations to S1 along the bundle skeletons during stimulations were generally greater than those in a resting state and from background regions. Consistent with the observations in Fig. 2 and Fig. 3, during tactile stimulations, the thalamus-S1 bundle in the contralateral hemisphere had the highest temporal correlation. Close comparisons reveal that the magnitude of temporal correlation along the thalamus-S1 skeletons in the contralateral hemisphere was approximately twice that in a resting state, and more than three times that for background white matter in a resting state. Detailed statistical comparisons in Tab. 2 show that the correlation along the thalamus-S1 bundle contralateral to the stimuli was significantly higher those at rest and for background white matter both during stimulation and at rest ($p<0.05$). The same difference can be also observed for the ponto-thalamus bundle. Of particular note, consistent with Fig. 2, the mean correlation along the thalamus-S1 bundle in the left hemisphere was significantly greater than that in the right hemisphere during right palm stimulations ($p<0.05$), but the difference was not significant during left palm stimulations.

Mean magnitudes of signals at the stimulus frequency along the skeleton connecting the thalamus to S1 and connecting the thalamus to pons are shown in Fig. 4 and Fig. 5 respectively. Similar to the findings from the correlation analysis above, the mean magnitude of stimulus frequency in BOLD signals along the contralateral thalamus-S1 skeleton during tactile stimulations was significantly greater than that in resting state for all the comparisons (Fig. 4), and along the contralateral ponto-thalamus skeleton was significantly greater than that in a resting state for all the comparisons as well (Fig. 5). Also along the contralateral thalamus-S1 skeleton, the magnitude was greater than the background white matter for all the comparisons both during stimulations and in resting state, and along the contralateral ponto-thalamus bundle, the magnitude was greater than the background white matter for 21 comparisons during stimulations and for all the comparisons in a resting state. There was also side-dependency in the mean magnitude along the thalamus-S1 skeletons (Fig. 4): right palm stimulations increased the magnitude along the TH-S1-L skeleton more than along the TH-S1-R skeleton in nine subjects, whereas left palm stimulations increased the magnitude along the TH-S1-R skeleton more than along the TH-S1-L skeleton only in six subjects.

Quantitative comparisons in the magnitude of signal at the stimulus frequency between the bundle skeletons and background white matter under both stimulation and resting state conditions are summarized in Tab. 3 and Tab. 4. It can be seen from Tab. 3 that the mean magnitudes along the bundle skeletons during stimulations were generally greater than those

in resting state and background regions. Consistent with the observations in Fig. 4 and Fig. 5, during tactile stimulations, the thalamus-S1 bundle in the contralateral hemisphere had the greatest magnitude, which was more than twice that in a resting state and about three times that for background white matter in a resting state. Tab. 4 shows the results of statistical tests, which reveal that the magnitudes along both the thalamus-S1 and the ponto-thalamus bundles contralateral to the stimuli were significantly greater than those at rest or in background white matter both during stimulations and at rest ($p<0.05$). The magnitude increases exhibited side-dependency statistically: the mean magnitude along the thalamus-S1 skeleton in the left hemisphere was significantly greater than that in the right hemisphere during right palm stimulations ($p<0.05$), but the difference was not significant during left palm stimulations. It should be noted that, although the background white matter exhibited magnitude increases during tactile stimulations, the somatosensory bundles achieved larger increases under stimulations.

Temporal variations and power spectra of BOLD signals averaged across the twelve subjects studied are shown in Fig. 6 and 7 respectively. It can be seen that, under both left and right palm stimulations, the BOLD signals in S1 and along the thalamus-S1 skeleton varied similarly to the stimulus waveform. The BOLD signals along the ponto-thalamus skeleton also exhibited periodic variations but with some noticeable time delay, likely due to different hemodynamic response along this bundle. These periodic variations are reflected by their much greater magnitudes at the stimulus frequency in Fig. 7. In contrast, the BOLD signals at rest did not show stimulus-related periodicity nor magnitude peak at the stimulus frequency, and the background had a very small magnitude peak localized at the stimulus frequency.

4 DISCUSSIONS

The existence of BOLD signals in brain white matter and their changes with stimulation has been controversial for some years. Logothetis et al. (2001) found that BOLD signals from cortex are primarily correlated with local field potentials instead of post-synaptic spiking outputs, which argues against the likely presence of BOLD signals in white matter. Conversely, Heeger and Ress (2002) later observed that BOLD signals are correlated mostly with spiking activity, which would allow a greater possibility that white matter may produce BOLD signals as well. A key question, though, is whether the power of BOLD signals in white matter, where vascular density is much smaller, can be detected by available fMRI technology. Recently there has been growing evidence that suggests the possibility of reliable detection of BOLD signals in white matter (e.g., Gawryluk et al., 2014). For instance, Tettamanti et al. (2002) demonstrated that BOLD signals in the genu of the corpus callosum may be detected by using Poffenberger paradigm, which was further confirmed by other groups (Weber et al., 2005; Gawryluk et al., 2009). Meanwhile, Fabri et al. (2011) found from a series of fMRI-based studies of functional topology of the corpus callosum that functional mapping of the corpus callosum may be consistently achieved by evoking activation through a suite of sensorimotor stimulations. In addition to the corpus callosum, BOLD activations in the internal capsule have also been reported (Mosier et al., 1999; Gawryluk et al., 2011). More recently, Astafiev et al. (2015) observed that the hemodynamic response in white matter possesses quite different profiles in patients with chronic mild

traumatic brain injury from healthy controls. Furthermore, by using steady stimulations with natural vision, Marussich et al. (2016) found that the optic radiations functionally reorganized and exhibited temporal correlations with the visual cortices during tasks.

While all these studies tend to support the contention that BOLD signals may be detectable in white matter, the current study presents further and perhaps more direct evidence of this notion. Compared to most other studies, which used conventional region-based methods designed for gray matter, we analyzed BOLD signals along specific fiber pathways that are presumably related to evoked functions. This tract-based analysis shares a similar concept with the TBSS approach (Smith et al., 2006) and thus in principle enhances both the sensitivity and specificity of signal detection. Our experiments have shown that, compared to the white matter background voxels, the fiber bundles connecting thalamus and S1 and thalamus to pons exhibit greater temporal correlations in BOLD signals with S1 in the contralateral hemisphere. Furthermore, the correlation strength and signal power of these bundles are approximately twice those in a resting condition.

The thalamus-S1 bundle directly connects sensory cortices in the gray matter so it is not unexpected that neural signals in this bundle exhibit significant correlations with the S1. It should be mentioned that white matter in this area contains functionally distinct fiber bundles with complicated spatial relations among each other, which may give rise to partial volume averaging effects in this bundle. Although this tended to reduce temporal correlations around the middle portion of the thalamus-S1 bundle, overall we found significantly increased temporal correlations along this bundle, which was consistent across the subjects studied.

The second bundle examined connected to the base of the pons. Unlike the thalamus-S1 bundle, this bundle starts from thalamus and stays farther away from gray matter as it goes inferiorly. Interestingly, BOLD signals along this distant white matter bundle also exhibit high correlations to the signals in the cortical gray matter. This phenomenon is probably made more obvious by the largely parallel nature of the neuronal fiber tracts in this bundle with much less interference from crossing bundles. Moreover, the signals in this white matter bundle are spared of influences from nearby gray matter, thus providing clearer evidence of the detectability of functional activities in white matter.

An interesting finding from this study was the lateralized responses in white matter. The observation that right palm stimulations evoked greater responses along the fiber bundle in the contralateral hemisphere while left palm stimulations evoked comparable responses in both hemispheres may be due to the fact that all the subjects in this study were right handed. In fact a similar phenomenon has been also observed in the cortex, which might be explained by differences in neural control or vascular distribution or both. Recently, Grabowska et al. (2012) found that, for both left- and right- handed subjects, activation was dominant in the contralateral hemisphere from movement of the preferred hand, whereas the activation was more balanced in both hemispheres from movements of the non-preferred hand. This study tends to suggest that the preferred hand is controlled primarily by the contralateral hemisphere, but the non-preferred hand is controlled by both hemispheres. Similar inferences can also be made for the lateralized sensory responses along the white

matter bundle observed in our study, which discounts the alternative explanation by vascular differences between the hemispheres.

Despite that this work, as well as a plethora of other studies (see Gawryluk et al., 2014 for review), demonstrated detectability of functional activations in white matter, the precise biophysical mechanisms of the signal origin remain unclear. Our earlier multi-echo imaging experiment showed that optimal contrast to noise in white matter occurs around TE ≈ T_2*, indicating the signal has the nature of blood oxygenation level dependency (Ding et al., 2016). This was further supported by the cerebrovascular CO_2 reactivity study by Rostrup et al. (2000), which revealed relative changes of BOLD signals in white matter from hypercapnia are similar to those in gray matter. In light of the close link between BOLD signals and neural spiking activities (Heeger and Ress, 2002; Nir et al., 2008), it may be possible that the BOLD signals in white matter are from spiking modulated vascular or metabolic responses (Wehrl et al., 2013; Driesen et al., 2013; Thompson et al., 2016), potentially via astrocyte signaling, just as in gray matter (Logothetis and Wandell, 2004).

Limitations

This study possesses a few inherent limitations. Most notably, BOLD signals are widely recognized as being susceptible to imaging artifacts, which adds to the difficulties of detecting weak BOLD signals in white matter (Bodurka et al., 2007). In this work, we employed a number of conventional procedures to ameliorate the effects of potential artifacts. First, we minimized subjects' head motion by carefully placing restricting pads within the head coil, and limited the displacement to be <1 mm and rotation <1° for all the twelve subjects studied. Second, the head motion was corrected using standard motion correction procedures in SPM. Third, we detrended BOLD signals to correct for potential signal drift due to instrumental imperfection. Another potential source of physiological noise arises from signal contamination from cardiac/respiratory rhythmic modulations. In our pilot work, we used RETROICOR (Glover et al., 2001) to correct the effect of cardiac/respiratory signals, but found that the changes in correlation measures were minimal. This agrees with an earlier report that contributions from cardiac signals are quite small (Cordes et al. 2001).

Several other confounding factors may also lead to biased estimation of true connectivity profiles within white matter. As alluded to earlier, white matter contains functionally distinct fiber bundles that run in parallel or across each other, and thus the effect of partial volume averaging can be severe given the spatial resolution used in this study (Van der Heuvel and Hulshoff, 2010). The partial volume effect was partly addressed in this work by extracting the largest principal components from each time series so that confounding signals from nearby bundles were reduced. Our assumption was that signals from relevant fibers are the principal contributor and that those from other fibers are orthogonal to them. While we have observed in our preliminary work that correlation with the largest principal components enhances connectivity metrics in white matter, it is not the ideal method for this purpose. There may be other methods, such as those based on independent component analysis (Beckmann et al., 2005) and wavelet analysis (Bullmore et al., 2004), that may improve performance. In addition, variable sensitivity among the subjects, as well as between different palms, may have some impact on the maps of signal correlation and power. Also,

imprecise processing procedures may bring in additional influences on measures of correlation and signal power. They may arise from errors in image registration, fiber tracking, bundle skeletonization, signal detrending, or spatial smoothing which tends to smear out BOLD signals. Another limitation comes from the relatively longer TR (=3s) and smaller number of volumes (=145) used in this study. This was due to a compromise between the spatial resolution, scanning time and effectiveness of the stimulation. However, with the rapid availability of multiband imaging (Xu et al., 2013), these parameters can be readily improved in our future work.

Finally, the background control used in this study, which was based on random selections of white matter voxels outside the bundles of interest, may have brought in some biases. We emphasize, however, that there are no absolutely fair ways of choosing the background control for this purpose. Ideally, a bundle not involved in tactile sensation, preferably with the same homogeneity profile of the magnetic field, should be used as the control; but it is very difficult, if not impossible, to determine which one is truly uninvolved (even indirectly). Choosing a bundle with least correlation to S1 would be a bias too. The use of random white matter voxels in this work might indeed contain voxels that were involved in tactile sensation, which would reduce the magnitudes of the results we report. Furthermore, 1000 random samples translated to much higher SNR than the skeletons, which posed another disadvantage, though this could be offset somewhat by less coherent smoothing of the background. Notwithstanding the limitation on the background control, our hypothesis was substantiated primarily by increased correlation strength and signal power from resting state and lateralized responses to stimuli, and to a lesser extent by the difference from the background control.

5 CONCLUSION

To explore whether BOLD signals in brain white matter are related to neural activity, somatosensory stimulation of the palms of different hands was performed, and temporal correlations between the primary somatosensory cortex and white matter bundles in the sensory pathways were analyzed and signal power along these bundles were examined. Quantitative analyses demonstrated that, overall, these specific fiber bundles exhibited significantly greater temporal correlation with the primary sensory cortex and signal power during palm stimulations than in a resting state, and greater than background white matter both during tactile stimulations and in a resting state. The temporal correlation and signal power were found to be twice those observed from the same bundle in a resting state. Resting state correlations between the cortex and connecting fibers were greater than with background white matter, and the signal power in the connecting fibers was greater than the background as well. There was a clear palm side dependency in the temporal correlation and signal power under stimulations. These findings demonstrate that BOLD signals in white matter may be related to evoked neural activities and may be detectable using sensitive methods.

Acknowledgments

This work is supported by NIH grants NS093669 (JCG), HD044073 (LEC), HD015052 (LEC) and MH064913 (LEC).

References

Astafiev SV, Shulman GL, Metcalf NV, Rengachary J, MacDonald CL, Harrington DL, Maruta J, Shimony JS, Ghajar J, Diwakar M, Huang MX, Lee RR, Corbetta M. Abnormal White Matter Blood-Oxygen-Level-Dependent Signals in Chronic Mild Traumatic Brain Injury. Neurotrauma. 2015; 32:1254–1271.

Beckmann CF, DeLuca M, Devlin JT, Smith SM. Investigations into resting-state connectivity using independent component analysis. Philos Trans Royal Soc Lond B Biol Sci. 2005; 360:1001–1013.

Biswal B, Yetkin FZ, Haughton VM, Hyde JS. Functional connectivity in the motor cortex of resting human brain using echo-planar MRI. Magn Reson Med. 1995; 34:537–541. [PubMed: 8524021]

Bodurka J, Ye F, Petridou N, Murphy K, Bandettini P. Mapping the MRI voxel volume in which thermal noise matches physiological noise-Implications for fMRI. Neuroimage. 2007; 34:542–549. [PubMed: 17101280]

Bullmore E, Fadili J, Maxim V, Sendur L, Whitcher B, Suckling J, Brammer M, Breakspear M. Wavelets and functional magnetic resonance imaging of the human brain. Neuroimage. 2004; 23:234–249.

Cordes D, Haughton VM, Arfanakis K, Carew JD, Turski PA, Moritza CH, Quigleya MA, Meyeranda ME. Frequencies contributing to functional connectivity in the cerebral cortex in “resting-state” data. AJNR Am J Neuroradiol. 2001; 22:1326–1333. [PubMed: 11498421]

D’Arcy RCN, Hamilton A, Jarmasz M, Sullivan SG, Stroink G. Exploratory data analysis reveals visuovisual interhemispheric transfer in functional magnetic resonance imaging. Magn Reson Med. 2006; 55:952–958. [PubMed: 16506159]

Ding Z, Gore JC, Anderson AW. Classification and quantification of neuronal fiber pathways using diffusion tensor MRI. Magn Reson Med. Apr; 2003 49(4):716–21. [PubMed: 12652543]

Ding Z, Newton AT, Xu R, Anderson AW, Morgan VL, Gore JC. Spatio-temporal correlation tensors reveal functional structure in human brain. PLoS One. 2013; 8:e82107. [PubMed: 24339997]

Ding Z, Xu R, Bailey SK, Wu TL, Morgan VL, Cutting LE, Anderson WA, Gore JC. Visualizing functional pathways in the human brain using correlation tensors and magnetic resonance imaging. Magnetic Resonance Imaging. 2016; 34(1):1–37. [PubMed: 26485295]

Driesen NR, McCarthy G, Bhagwagar Z, Bloch M, Calhoun V, D’Souza DC, Gueorguieva R, He G, Ramachandran R, Suckow RF, Anticevic A, Morgan PT, Krystal JH. Relationship of resting brain hyperconnectivity and schizophrenia-like symptoms produced by the NMDA receptor antagonist ketamine in humans. Mol Psychiatry. 2013; 18(11):1199–1204. [PubMed: 23337947]

Fabri M, Polonara G, Mascioli G, Salvolini U, Manzoni T. Topographical organization of human corpus callosum: An fMRI mapping study. Brain Res. 2011; 1370:99–111. [PubMed: 21081115]

Fox MD, Raichle ME. Spontaneous fluctuations in brain activity observed with functional magnetic resonance imaging. Nat Rev Neurosci. 2007; 8:700–711. [PubMed: 17704812]

Friman O, Farnebäck G, Westin CF. A Bayesian Approach for Stochastic White Matter Tractography. IEEE Transactions on Medical Imaging. 2006; 25(8):965–978. [PubMed: 16894991]

Gawryluk JR, Brewer KD, Beyea SD, D’Arcy RCN. Optimizing the detection of white matter fMRI using asymmetric spin echo spiral. Neuroimage. 2009; 45:83–88. [PubMed: 19084071]

Gawryluk JR, Mazerolle EL, Brewer KD, Beyea SD, D’Arcy RCN. Investigation of fMRI activation in the internal capsule. BMC Neurosci. 2011; 12(56):1–7. [PubMed: 21208416]

Gawryluk JR, Mazerolle EL, D’arcy RCN. Does functional MRI detect activation in white matter? A review of emerging evidence, issues, and future directions. Front Neurosci. 2014; 8(239):1–12. [PubMed: 24478622]

Glover GH, Li TQ, Ress D. Image-based method for retrospective correction of physiological motion effects in fMRI: RETROICOR. Magn Reson Med. 2000; 44:162–167. [PubMed: 10893535]

Gore JC. Principles and practice of functional MRI of the human brain. J Clin Invest. 2003; 112:4–9. [PubMed: 12840051]

Grabowska A, Gut M, Binder M, Forsberg L, Rymarczyk K, Urbanik A. Switching handedness: fMRI study of hand motor control in right-handers, left-handers and converted left-handers. Acta Neurobiol Exp. 2012; 72(4):439–451.

Heeger DJ, Ress D. What does fMRI tell us about neuronal activity? Nat Rev Neurosci. 2002; 3:142–151. [PubMed: 11836522]

Jones DK, Cercignani M. Twenty-five pitfalls in the analysis of diffusion MRI data. NMR Biomed. 2010; 23:803–820. [PubMed: 20886566]

Logothetis NK, Pauls J, Augath M, Trinath T, Oeltermann. Neurophysiological investigation of the basis of the fMRI signal. Nature. 2001; 412:150–157. [PubMed: 11449264]

Logothetis NK, Wandell BA. Interpreting the BOLD signal. Annu Rev Physiol. 2004; 66:735–769. [PubMed: 14977420]

Maldjian JA, Laurienti PJ, Kraft RA, Burdette JH. An automated method for neuroanatomic and cytoarchitectonic atlas-based interrogation of fmri data sets. NeuroImage. 2003; 19:1233–1239. [PubMed: 12880848]

Marussich L, Lu KH, Wen H, Liu Z. Mapping white-matter functional organization at rest and during naturalistic visual perception. NeuroImage. 2016 in press.

Mazerolle EL, Gawryluk JR, Dillen KN, Patterson SA, Feindel KW, Beyea SD, Stevens MT, Newman AJ, Schmidt MH, D'Arcy RCN. Sensitivity to white matter FMRI activation increases with field strength. PLoS One. 2013; 8:e58130. [PubMed: 23483983]

Mosier KM, Liu WC, Maldjian JA, Shah R, Modi B. Lateralization of cortical function in swallowing: A functional MR imaging study. Am J Neuroradiol. 1999; 20:1520–1526. [PubMed: 10512240]

Nir Y, Dinstein I, Malach R, Heeger DJ. BOLD and spiking activity. Nat Neurosci. 2008; 11(5):523–524. [PubMed: 18437185]

Nonaka H, Akima M, Hatori T, Nagayama T, Zhang Z, Ihara F. Microvasculature of the human cerebral white matter: arteries of the deep white matter. Neuropathology. 2003a; 23:111–118. [PubMed: 12777099]

Nonaka H, Akima M, Hatori T, Nagayama T, Zhang Z, Ihara F. The microvasculature of the cerebral white matter: arteries of the subcortical white matter. J Neuropathol Exp Neurol. 2003b; 62:154–161. [PubMed: 12578225]

Ogawa S, Lee TM, Kay AR, Tank DW. Brain magnetic resonance imaging with contrast dependent on blood oxygenation. Proc Natl Acad Sci USA. 1990; 87:9868–9872. [PubMed: 2124706]

Raichle ME, MacLeod AM, Snyder AZ, Powers WJ, Gusnard DA, Shulman GL. A default mode of brain function. Proc Natl Acad Sci USA. 2001; 98:676–682. [PubMed: 11209064]

Rostrup E, Law I, Blinkenberg M, Larsson HBW, Born AP, Holm S, Paulson OB. Regional differences in the CBF and BOLD responses to hypercapnia: a combined PET and fMRI study. NeuroImage. 2000; 11:87–97. [PubMed: 10679182]

Smith SM, Jenkinson M, Johansen-Berg M, Rueckert D, Nichols TE, Mackayn CE, Watkins KE, Ciccarelli O, Cader MZ, Matthews PM, Behrens TEJ. Tract-based spatial statistics: Voxelwise analysis of multi-subject diffusion data. NeuroImage. 2006; 31:1487–1505. [PubMed: 16624579]

Tettamanti M, Paulesu E, Scifo P, Maravita A, Fazio F, Perani D, Marzi CA. Interhemispheric transmission of visuomotor information in humans: fMRI evidence. J Neurophys. 2002; 88:1051–1058.

Thompson GJ, Riedl V, Grimmer T, Drzezga A, Herman P, Hyder F. The whole-brain "global" signal from resting state fMRI as a potential biomarker of quantitative state changes in glucose metabolism. Brain Connectivity. 2016; 6(6):435–447. [PubMed: 27029438]

Van den Heuvel MP, Hulshoff Pol HE. Exploring the brain network: A review on resting-state fMRI functional connectivity. Eur Neuropsychopharmacol. 2010; 20(8):519–534. [PubMed: 20471808]

Weber B, Treyer V, Oberholzer N, Jaermann T, Boesiger P, Brugger P, Regard M, Buck A, Savazzi S, Marzi CA. Attention and interhemispheric transfer: a behavioral and fMRI study. J Cogn Neurosci. 2005; 17:113–123. [PubMed: 15701243]

Wehrl HF, Hossain M, Lankes K, Liu C, Bezrukov I, Martirosian P, Pichler BJ. Simultaneous PET-MRI reveals brain function in activated and resting state on metabolic, hemodynamic and multiple temporal scales. Nature Medicine. 2013; 19(9):1184–1189.

Wu TL, Wang F, Anderson AW, Chen LM, Ding ZH, Gore JC. Effects of anesthesia on resting state BOLD signals in white matter of non-human primates. Magnetic Resonance Imaging. 2016; 34(9): 1235–1241. [PubMed: 27451405]

Xu J, Moeller S, Auerbach EJ, Strupp J, Smith SM, Feinberg DA, Yacoub E, Uğurbil K. Evaluation of slice accelerations using multiband echo planar imaging at 3T. Neuroimage. 2013; 83:991–1001. [PubMed: 23899722]

Yarkoni T, Barch DM, Gray JR, Conturo TE, Braver TS. BOLD correlates of trial-by-trial reaction time variability in gray and white matter: a multi-study fMRI analysis. PLoS One. 2009; 4:e4257. [PubMed: 19165335]

Highlights

- Tactile stimulations induced functional signal changes along projection pathways
- Temporal correlation and signal power from stimulations were twice resting state
- Correlation and signal power in projection pathways were stronger than background
- Changes of signals in projection pathways depended on the side of stimulations

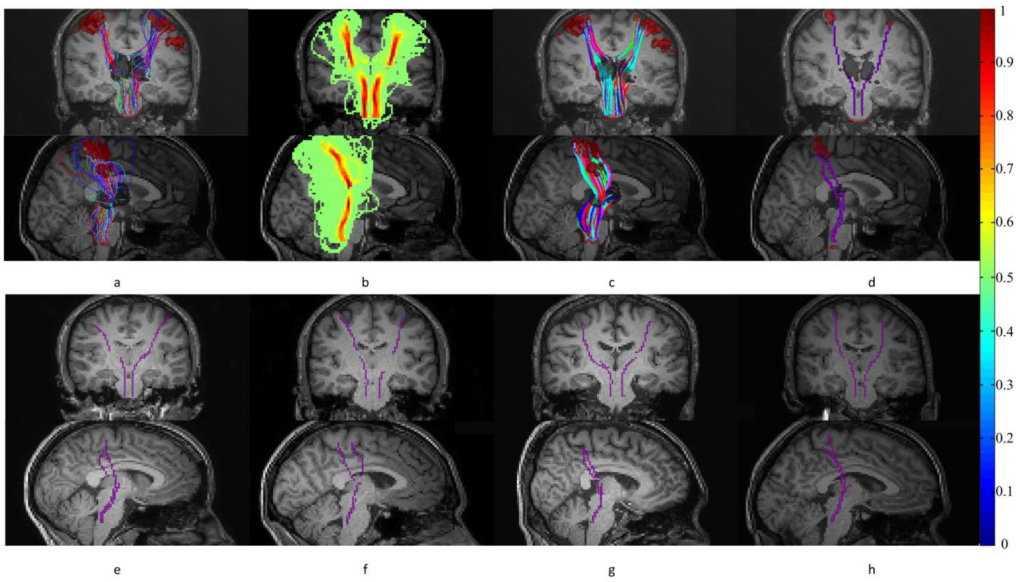

Figure 1.

Tracking and skeletonization of the projection pathways. (a) Probabilistic tracking of fibers from thalamus to S1 (and pons). (b) Probability density of fibers connecting thalamus and S1 (and pons). (c) Streamlines generated by backtracking from S1 (and pons) to thalamus. (d) Skeletons of fiber bundles connecting thalamus and S1 (and pons). First and second rows are coronal and sagittal views respectively. (e–h) Representative skeletons from four other subjects shown in coronal and sagittal views. Note that the colorbar on the far right is for panel (b).

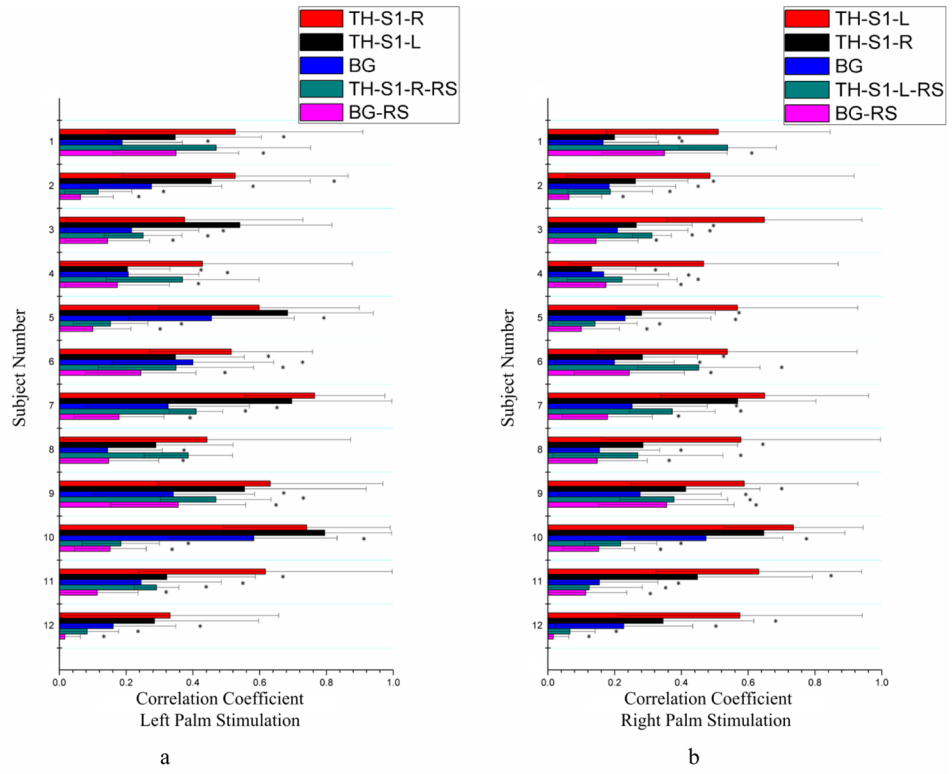

Figure 2.

Comparisons of mean correlations between signals along the bundle skeleton connecting the thalamus to S1 and S1 for tactile stimulation and resting state conditions. Background (BG) included 1000 random white matter voxels outside the fiber bundles connecting the thalamus and S1 (and pons). Left (a) and right (b) columns are for left and right palm stimulations respectively. *denotes $p<0.05$. See text for explanations of the abbreviations.

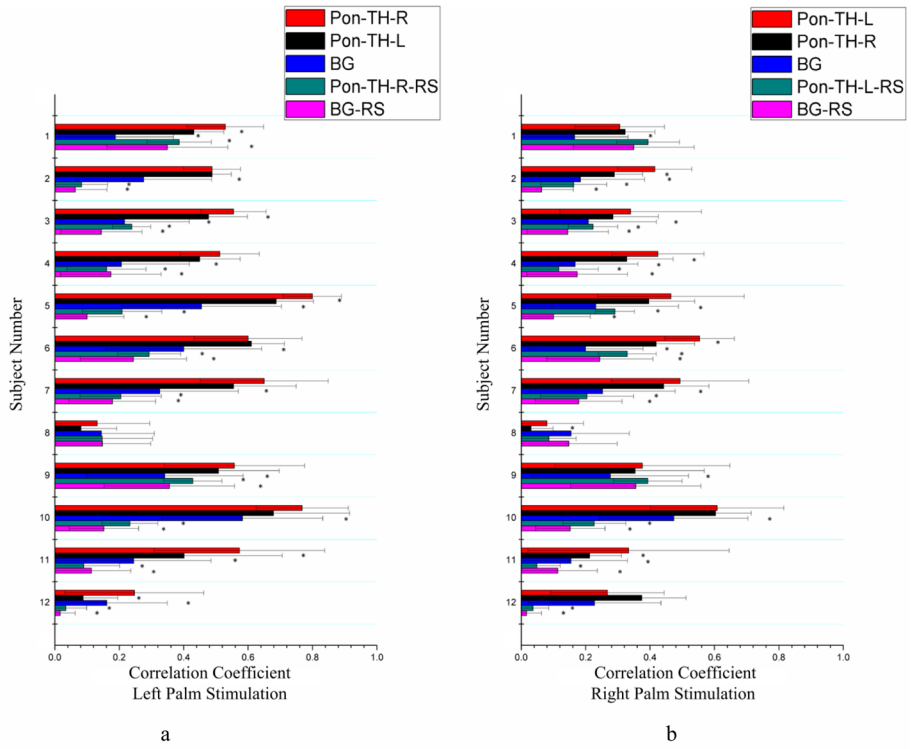

Figure 3.

Comparisons of mean correlations between signals along the bundle skeleton connecting the thalamus to the pons and the pons for stimulation and resting state conditions. BG area included 1000 random white matter voxels outside the fiber bundles connecting the thalamus and pons (and S1). Left (a) and right (b) columns are for left and right palm stimulations respectively. *denotes $p<0.05$. See text for explanations of the abbreviations.

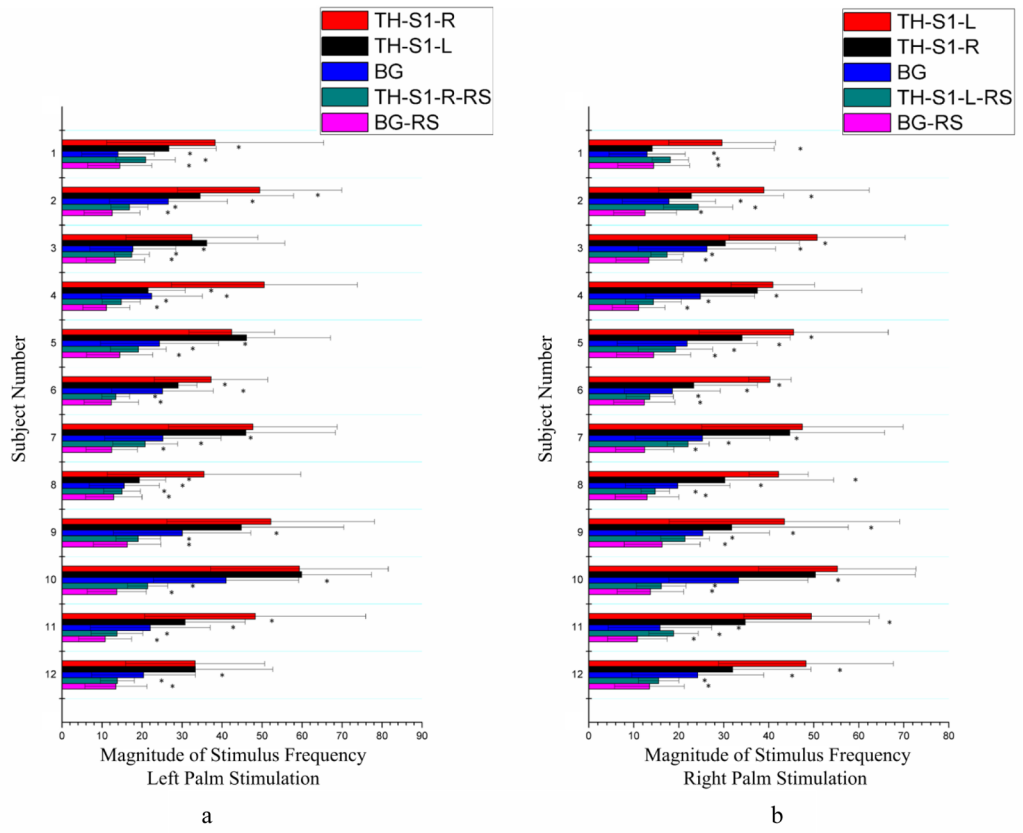

Figure 4.

Comparisons of mean signal magnitude at stimulus frequency along the bundle skeleton connecting the thalamus and the S1 area between tactile stimulation and resting state conditions. Left (a) and right (b) columns are for left and right palm stimulations respectively. *denotes $p<0.05$. See text for explanations of the abbreviations.

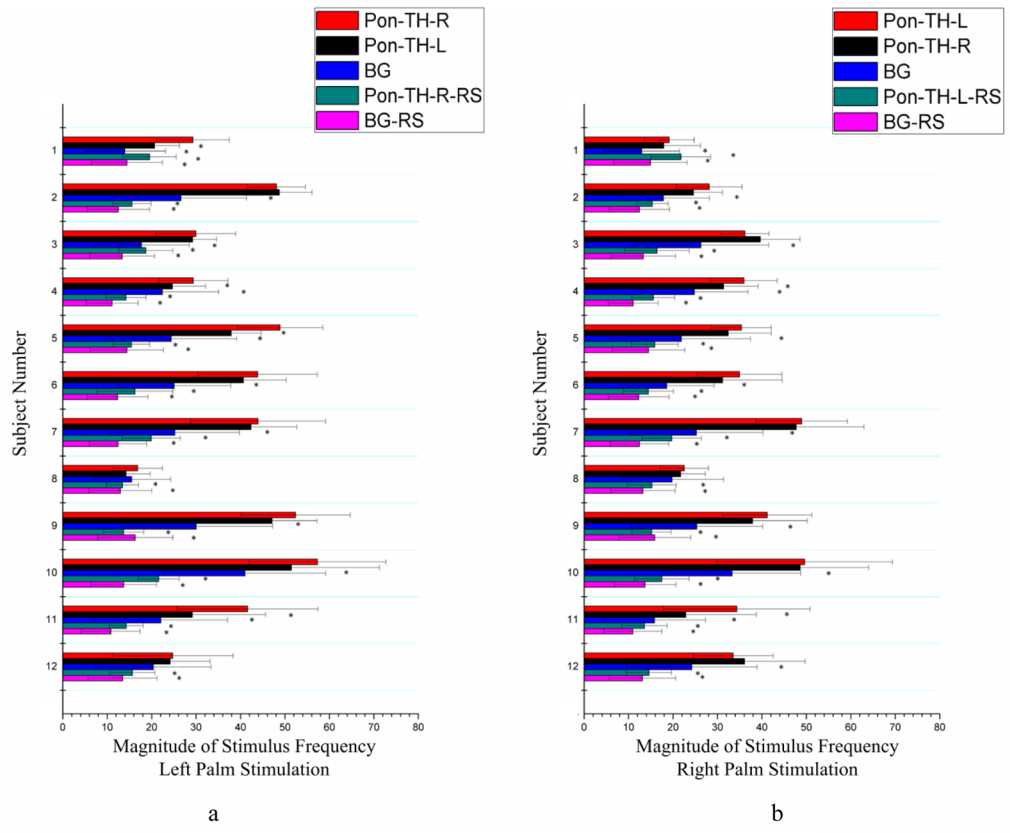

Figure 5.

Comparisons of mean signal magnitude at stimulus frequency along the bundle skeleton connecting the thalamus and the pons area between tactile stimulation and resting state conditions. Left (a) and right (b) columns are for left and right palm stimulations respectively. *denotes $p<0.05$. See text for explanations of the abbreviations.

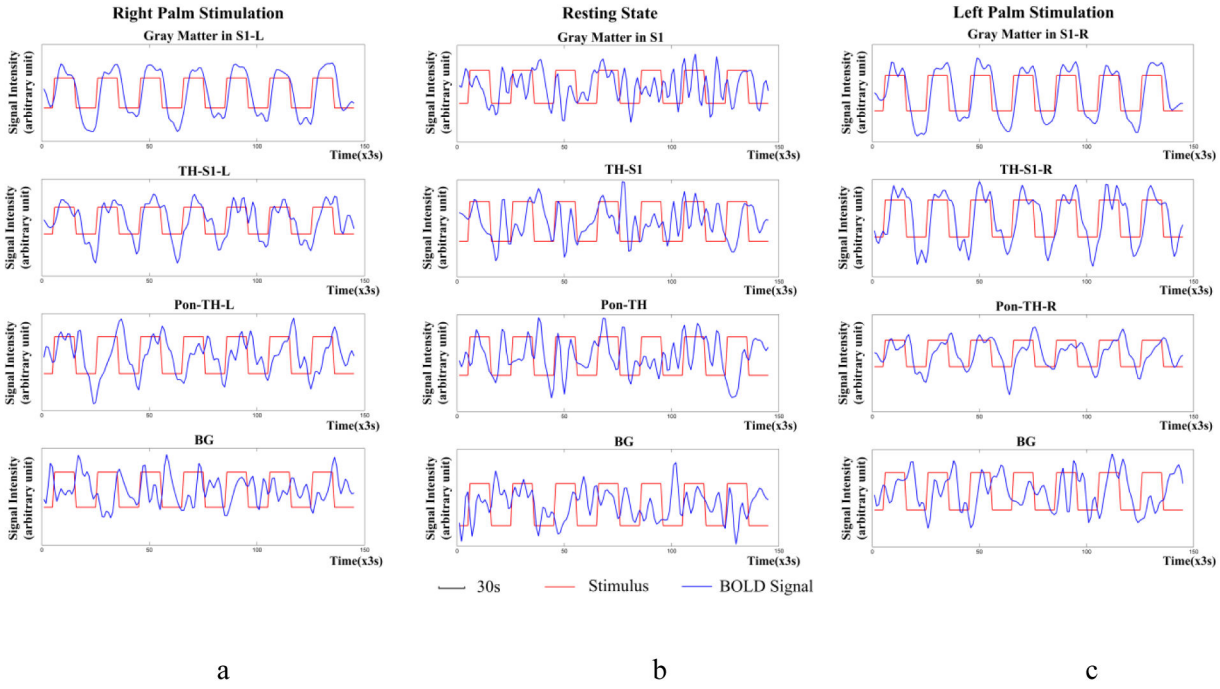

Figure 6.

Temporal variations of BOLD signals averaged across the twelve subjects studied. From top to bottom rows are mean BOLD signals in S1, along the bundle skeleton connecting thalamus and S1, along the bundle skeleton connecting thalamus and pons, and background respectively. From left to right columns are right palm stimulations (a), resting state condition (b) and left palm stimulations (c) respectively. The signal intensity is in arbitrary unit and red and blue curves represent stimulus and BOLD signal respectively. Note that, unlike stimulation conditions, BOLD signals in the resting state contain no stimulus-related periodicity.

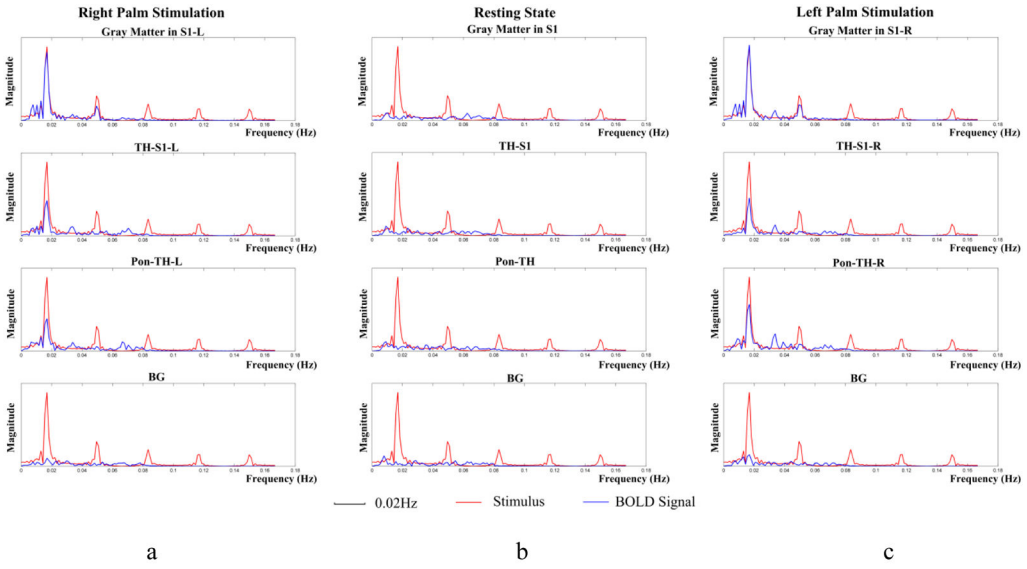

Figure 7.
Power spectra of mean BOLD signals in Figure 6.

Table 1

Mean and standard deviation of temporal correlations between thalamus-S1 and ponto-thalamus skeletons with S1. Note that BOLD signals in the S1 of the right and left hemisphere and both hemispheres are used as the basis of correlation for the left and right palm stimulations and resting state condition respectively.

Stimulations	Region	Mean	Standard deviation
Left palm stimulations	TH-S1-L	0.5296	0.2755
	TH-S1-R	0.6271	0.2065
	Pon-TH-L	0.5130	0.2410
	Pon-TH-R	0.6299	0.2694
	BG	0.3111	0.1540
Right palm stimulations	TH-S1-L	0.6721	0.1218
	TH-S1-R	0.3701	0.1849
	Pon-TH-L	0.4195	0.1664
	Pon-TH-R	0.3594	0.1593
	BG	0.2298	0.0943
Resting state condition	TH-S1-L	0.2871	0.1588
	TH-S1-R	0.3090	0.1490
	Pon-TH-L	0.2158	0.1323
	Pon-TH-R	0.2153	0.1271
	BG	0.1736	0.1084

Table 2

Statistical comparisons of temporal correlations during tactile stimulations. Boldfaced numbers denote p<0.05.

Stimulation	Region A	Region B	p-value
Left palm stimulations	TH-S1-R	TH-S1-L	0.3373
		BG	**0.0003**
		TH-S1-R-RS	**0.0003**
		BG-RS	**<0.0001**
	Pon-TH-R	Pon-TH-L	0.2747
		BG	**0.0018**
		Pon-TH-R-RS	**0.0001**
		BG-RS	**0.0002**
Right palm stimulations	TH-S1-L	TH-S1-R	**0.0001**
		BG	**<0.0001**
		TH-S1-L-RS	**0.0001**
		BG-RS	**<0.0001**
	Pon-TH-L	Pon-TH-R	0.3761
		BG	**0.0024**
		Pon-TH-L-RS	**0.0017**
		BG-RS	**0.0010**

Table 3

Mean and standard deviation of the magnitude of stimulus frequency under tactile stimulation and resting state conditions.

Stimulations	Region	Mean	Standard deviation
Left palm stimulations	TH-S1-L	35.67	11.70
	TH-S1-R	43.89	8.56
	Pon-TH-L	34.18	12.14
	Pon-TH-R	38.85	12.47
	BG	23.70	7.17
Right palm stimulations	TH-S1-L	44.34	6.69
	TH-S1-R	32.14	9.65
	Pon-TH-L	34.99	9.07
	Pon-TH-R	32.67	9.86
	BG	22.16	5.50
Resting state condition	TH-S1-L	17.98	3.35
	TH-S1-R	17.19	3.01
	Pon-TH-L	16.27	2.35
	Pon-TH-R	16.53	2.72
	BG	13.15	1.51

Table 4

Statistical comparisons of the magnitude of stimulus frequency during tactile stimulations. Boldfaced numbers denote $p<0.05$.

Stimulation	Region A	Region B	p-value
Left palm stimulations	TH-S1-R	TH-S1-L	0.0622
		BG	**0.0063**
		TH-S1-R-RS	**<0.0001**
		BG-RS	**<0.0001**
	Pon-TH-R	Pon-TH-L	0.3631
		BG	**0.0173**
		Pon-TH-R-RS	**<0.0001**
		BG-RS	**<0.0001**
Right palm stimulations	TH-S1-L	TH-S1-R	**0.0016**
		BG	**<0.0001**
		TH-S1-L-RS	**<0.0001**
		BG-RS	**<0.0001**
	Pon-TH-L	Pon-TH-R	0.5546
		BG	**0.0004**
		Pon-TH-L-RS	**<0.0001**
		BG-RS	**<0.0001**